Available online at www.sciencedirect.com
ScienceDirect
Journal of the European Ceramic Society 26 (2006) 3113–3121
www.elsevier.com/locate/jeurceramsoc

Processing, microstructure and mechanical properties of directionally-solidified Al_2O_3–$Y_3Al_5O_{12}$–ZrO_2 ternary eutectics

J.I. Peña [a,*], M. Larsson [a], R.I. Merino [a], I. de Francisco [a], V.M. Orera [a], J. LLorca [b], J.Y. Pastor [b], A. Martín [b], J. Segurado [b]

[a] *Instituto de Ciencia de Materiales de Aragón, C.S.I.C.-Universidad de Zaragoza, 50018 Zaragoza, Spain*
[b] *Department of Materials Science. Polytechnic University of Madrid, E.T.S. de Ingenieros de Caminos, 28040 Madrid, Spain*

Received 11 April 2005; received in revised form 24 October 2005; accepted 29 October 2005
Available online 20 December 2005

Abstract

Rods of 1–2 mm diameter of $Al_2O_3/Y_3Al_5O_{12}/ZrO_2$ in the ternary eutectic composition (65 mol% Al_2O_3, 19 mol% ZrO_2, 16 mol% Y_2O_3) were grown by the laser-heated floating-zone method at growth rates between 10 and 1000 mm/h. At low growth rates the rods presented a Chinese script microstructure formed by an interpenetrating network of Al_2O_3 (40%) and $Y_3Al_5O_{12}$ (42%) domains of similar size, with smaller cubic Y_2O_3-stabilized ZrO_2 (18%) domains at the $Al_2O_3/Y_3Al_5O_{12}$ interfaces. Compressive residual stresses of 200 MPa were measured in the alumina phase by piezo-spectroscopy and their thermo-elastic origin was validated by self-consistent simulations. The phase spacing and the residual stresses decreased with increasing growth rate and this influenced the hardness and the fracture toughness. The fine and homogeneous microstructure of the ternary eutectic rods led to an outstanding flexure strength of 2.3 GPa at ambient temperature, which was retained up to 1473 K, and then decreased rapidly to 1.2 GPa at 1700 K.

Keywords: Microstructure-final; Strength; Fracture; Directional solidification; Eutectics; Al_2O_3; ZrO_2; $Y_3Al_5O_{12}$

1. Introduction

Directionally-grown sapphire-based eutectics present excellent creep and oxidation resistance as well as chemical stability at high temperature in aggressive environments,[1] and this has prompted the search and development of new eutectic ceramic oxides for structural applications at elevated temperatures. The research was focused mainly on binary eutectics of the families Al_2O_3/ZrO_2 and Al_2O_3/Y_2O_3, where the relationship between microstructure and mechanical properties on the one hand[2–6] and between growth parameters and microstructure on the other[7–10] is well established. For example, $Al_2O_3/Y_3Al_5O_{12}$ (YAG) eutectics with a fine microstructure formed by an interpenetrating network of both phases attained an excellent bending strength of 1.9 GPa at ambient temperature, which decreased only to 1.5 GPa at 1900 K. However, their toughness is very low ($\approx$2 MPa m$^{1/2}$),[5,6] and this leads to materials whose strength was very sensitive to the development of micron-sized surface defects and prone to brittle fracture. Other sapphire-based pseudo-binary eutectics, such as $Al_2O_3/ZrO_2(Y_2O_3)$, present better fracture toughness ($\approx$4–5 MPa m$^{1/2}$) and excellent mechanical properties at ambient temperature although the strength retention at high temperatures was poorer, presumably because cubic ZrO_2 presents lower creep resistance than YAG.[2–4]

Further improvements in the mechanical properties can be expected in other regions of the Al_2O_3–ZrO_2–Y_2O_3 phase diagram, and the $Al_2O_3/ZrO_2/Y_2O_3$ ternary eutectic composition has attracted attention recently. Calderón-Moreno manufactured ternary eutectic pellets of this composition using rapid solidification techniques,[11] and Lee et al.[12] and Waku et al.[13] have reported some preliminary results on the microstructure and mechanical properties of fibers and bulk samples grown by directional-solidification. However, no comprehensive study of the relationship between the growth parameters, the microstructure and the mechanical properties of ternary eutectics has yet been carried out and this was the main objective of this investigation. $Al_2O_3/ZrO_2/Y_2O_3$ ternary eutectic rods were grown

* Corresponding author. Tel.: +34 976761958; fax: +34 976761957.
E-mail address: jipena@unizar.es (J.I. Peña).

0955-2219/$ – see front matter © 2005 Elsevier Ltd. All rights reserved.
doi:10.1016/j.jeurceramsoc.2005.11.005

by the laser-heated floating-zone (LFZ) method at growth rates between 10 and 1000 mm/h. The processing conditions were optimized to manufacture rods with homogeneous microstructure throughout the sample, and the microstructural characterization was completed with the measurement of the residual stress in the Al_2O_3 phase. The hardness and fracture toughness were measured in rods grown at different rates and the evolution of the flexure strength with temperature up to 1700 K was determined in one selected material. The results of the mechanical tests and of the microstructural characterization were used to establish the influence of the microstructure (and hence of the processing conditions) on the mechanical behavior of the ternary eutectics.

2. Experimental techniques

Commercially available powders were mixed in the ternary eutectic composition (65 mol% Al_2O_3, 19 mol% ZrO_2, 16 mol% Y_2O_3) given by Lakiza and Lopato.[14] The powders used were 99.99% aluminum oxide from Sasol North America Inc., 8% yttria stabilized zirconia (TZ-8YS) from Tosoh Corporation and 99.99% yttrium oxide from Aldrich Chemical Company Inc. Since the zirconia powder was already stabilized with yttria, the addition of yttrium oxide was smaller than if pure zirconia had been used (14.3% mol). A small amount of polyvinyl alcohol was added as a binder to the mixed powder and rods were prepared by isostatic cold-pressing at 200 MPa for 3 min. The green bodies were heat treated for 1 h at 800 K to burn off the organic binder and then sintered at 1773 K for 12 h to obtain the precursor rods. They were directionally-solidified from the melt by the LFZ method as described elsewhere[15] to obtain eutectic crystals of 1–2 mm in diameter. The dependence of microstructure on the processing parameters was studied by varying systematically the growth rate (from 10 to 1000 mm/h) and the rotation speed of the rods (from 0 to 200 rpm). Usually the rotation direction of the precursor rod was contrary to that of the grown rod. A molten zone of length of ≈1.5 times the rod diameter was maintained by adjusting the laser power input. Upward solidification was chosen because this led to higher stability of the molten zone than downward growth. Reductions in rod diameter were achieved when necessary by setting a lower speed to the precursor than to the grown rod. Some experiments were ended abruptly by turning off the laser and the pull speed to study the shape of the solidification front. This gave an air-quenched molten zone of extremely fine phase size, which is easily distinguished from the rod grown under standard conditions. Longitudinal and transversal sections of the rods were examined under the scanning electron microscope to determine the spatial distribution and size of the phases.

The Vickers hardness was measured following the ASTM C1327–99 Standard[16] using a Matsuzawa MXT50 microhardness indenter. The specimens were loaded with 4.9 N for 15 s and at least ten valid microindentations were made in each sample. The size of the indentation mark as well as the length of the cracks emanating from the indentation corners were measured immediately after each indentation. The flexure strength of the rods was measured from 300 to 1700 K by three-point bend tests in air in an alumina fixture of 8.5 mm loading span. The specimen and the loading fixture were placed in a furnace and loaded through two alumina rods connected to the actuator and to the load cell, respectively, of a servo-mechanical testing machine (model 4505, Instron Ltd, High Wycombe, UK). The specimen was held at the test temperature for 30 min before testing. The tests were performed under stroke control at a cross-head speed of 50 μm/min. The load-displacement curves were linear for all the materials and temperatures, and the flexure strength was computed from the maximum load in the test according to the Strength of Materials theory for a Bernoulli elastic beam of circular section.

Piezo-spectroscopic measurements were made at room temperature using an optical spectrometer (Model XY, DILOR, Lille, France) with a diode array multichannel detector.[17] The Cr^{3+} emission spectra of ruby from chromium traces in the starting powders, were collected at room temperature using an Ar^+ laser as the excitation source. An unstressed sapphire single crystal was used to derive the reference spectrum. The hydrostatic component of the residual stresses in the Al_2O_3 phase was determined from the shift in the position of the R2 line of ruby (14433 cm^{-1} at 300 K) in rods grown at different rates.

3. Results and discussion

3.1. Microstructure

The directionally-solidified rods were white with a smooth surface. Those grown at the lowest rates were opalescent whereas the rods grown at the highest speeds were glossy and shiny. Rotation did not modify their appearance. The quenched zone created by switching off the laser power was translucent and very fragile. The samples grown at the highest rate (1000 mm/h) presented a skin-core structure clearly visible in the transverse cross section, and the skin had the same appearance as in the quenched zones. Obviously, these changes in the optical appearance were related to variations in the phase size.

The presence of pores in the directionally-solidified rods was one of the main concerns because of their influence on the mechanical properties. Fig. 1 shows the changes in pore morphology with the growth rate and the rotation speed. No porosity was detected in the rods grown at low rates (<50 mm/h) (Fig. 1a) but small pores, evenly distributed throughout the cross section, were found in those grown at 50 mm/h (Fig. 1b). Larger pores were found ubiquitously in all the samples grown at higher rates even if the precursors were fully dense. The melt viscosity was very high, probably associated to the ternary eutectic composition rich on $Y_3Al_5O_{12}$ (YAG).[18] In fact, molten YAG presents high viscosity values as compared for example, with those of Al_2O_3. Consequently, the gas cavities have no time to reach the melt surface and escape in the rods grown at high rates, remained trapped in the solid phase. Large cavities in the rod centre appeared at 300 mm/h (Fig. 1c), while pores of intermediate size were found between the outer edge and the centre of the rod at 1000 mm/h (Fig. 1d). Vigorous counter rotation (200 rpm) of the precursor and grown rods did not eliminate the

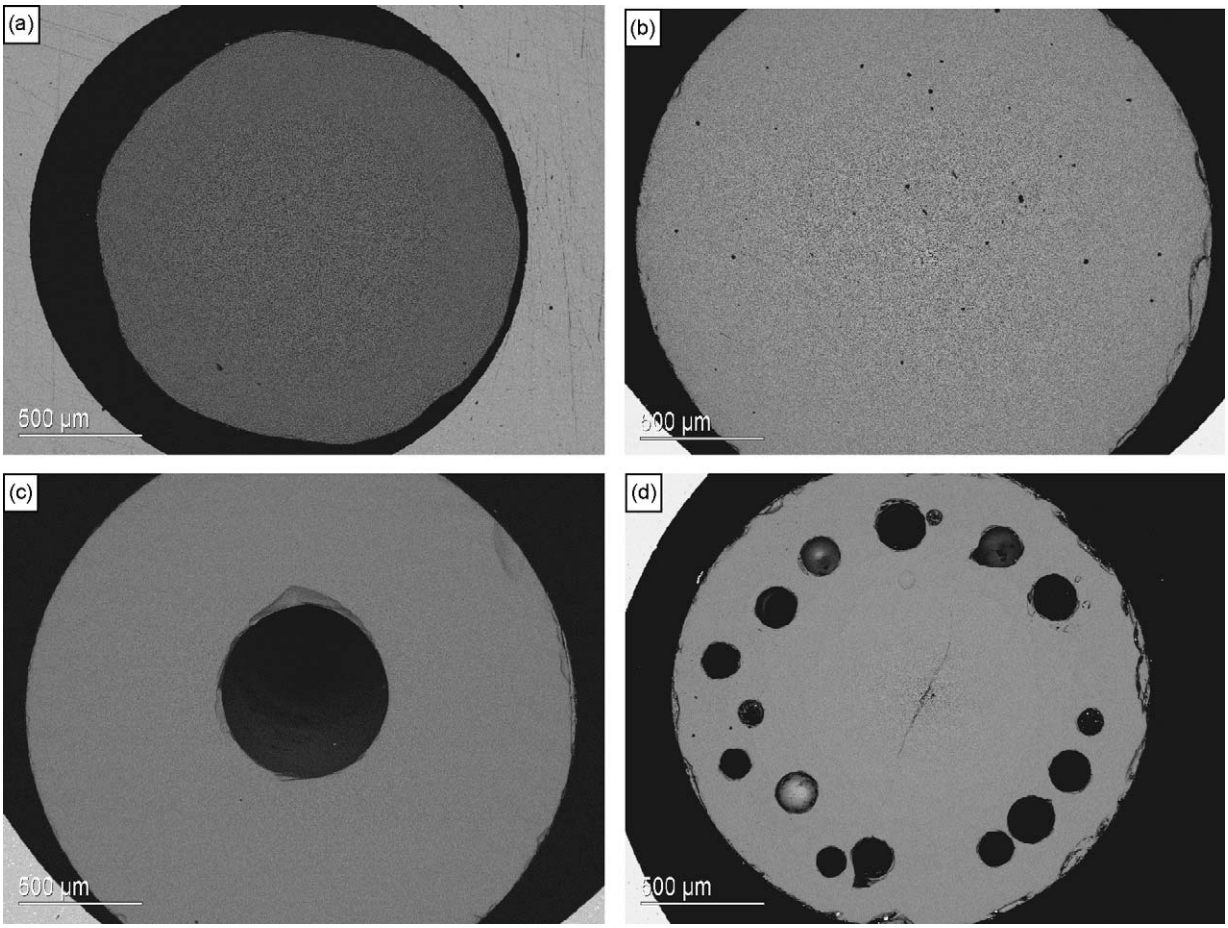

Fig. 1. Scanning electron micrographs of transversal cross sections of Al_2O_3–ZrO_2–Y_2O_3 ternary eutectics grown at different rates: (a) 10 mm/h; (b) 50 mm/h; (c) 300 mm/h, ±200 rpm and (d) 1000 mm/h.

pores although it forced the aggregation of pores in the core to collapse at the rod axis while those near the surface were pushed towards the rod surface and eventually escaped.

Representative micrographs of the transverse sections of ternary eutectics grown at 10, 50, 300 and 1000 mm/h are shown in Fig. 2a–d. The microstructure of the rods grown at 10 mm/h showed three evenly distributed phases, Al_2O_3, cubic Y_2O_3-stabilized ZrO_2 (YSZ), and YAG as shown by X-ray diffraction analysis. Image analysis of SEM images of the low growth rate samples leads to approximated volume fractions of 0.40, 0.18 and 0.42, respectively which coincides with that expected for eutectic composition. The YAG domains of different size were embedded in a matrix formed by a mixture of Al_2O_3 and YSZ domains (Fig. 2a). The YSZ domains tended to appear at the Al_2O_3–YAG interfaces and were much smaller than the Al_2O_3 and YAG ones. The eutectic morphology changed at 50 mm/h (Fig. 2b), and the YAG domains were interconnected while the Al_2O_3 and YSZ phases formed the dispersed phase. These results are in good agreement with those reported by Lee et al.,[12] who observed a similar change in the morphology between samples grown at low and at high rates. This morphology (also named Chinese script microstructure) was maintained at the higher growth rates (Fig. 2c and d). The size of the domains decreased rapidly with growth rate and no YSZ domains could be resolved by scanning electron microscope in the samples grown at 1000 mm/h (Fig. 2d). The analysis of the longitudinal sections (Fig. 2e) showed that the Al_2O_3 and YAG domains were elongated along the growth axis while the YSZ regions nucleated at the Al_2O_3/YAG interfaces. Rotation did not modify significantly the microstructure morphology.

The interface between the quenched and the normally solidified material is shown in Fig. 3a, and a detail of the solidification interface in Fig. 3b. The YAG phase is being projected into the melt as a result of the high entropy of melt of YAG which plays the leading role in the eutectic solidification.[1] The solidification front was macroscopically curved and convex towards the melt in the rods grown at 10 mm/h (Fig. 3a) and the processing effort was directed towards obtaining a flat solidification front, which is expected to yield a more homogeneous microstructure than a curved one. According to the Young and Chait model,[19] this can be done by increasing the growth rate but this increased the tendency to develop pores. Rotation can also help to flatten the solidification front but its influence in this material was negligible. Of course, rotation led to a more symmetrically shaped solidification front because of the homogeneous distribution of heating but it also introduced banding in the microstructure. Similar effects were reported by de Francisco et al.[20] in the Al_2O_3–$ZrO_2(Y_2O_3)$ binary eutectics, and the mechanical char-

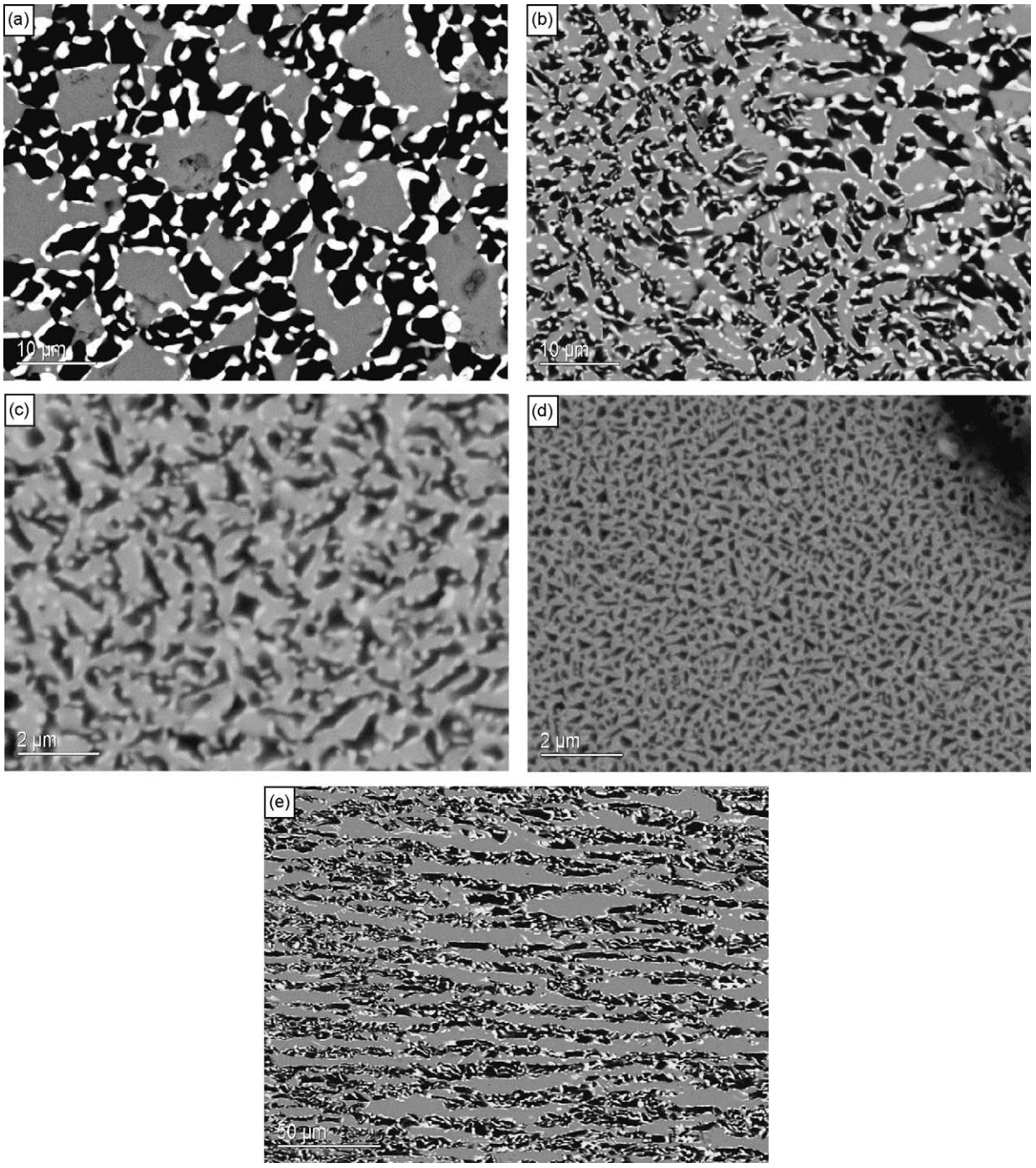

Fig. 2. Back-scattered scanning electro micrographs of the transversal cross sections of Al_2O_3–ZrO_2–Y_2O_3 ternary eutectics grown at different speeds and without rotation: (a) 10 mm/h; (b) 50 mm/h; (c) 300 mm/h; (d) 1000 mm/h and (e) back-scattered scanning electro micrograph of the longitudinal cross section of the ternary eutectic grown at 10 mm/h The black phase is alumina, the grey one YAG and the white one YSZ.

acterization was made in rods grown without rotation because banding increases scatter in the mechanical properties.[3]

3.2. Residual stresses

Thermo-elastic residual stresses develop upon solidification on account of the thermal expansion coefficient mismatch among the component phases. The average value of the alumina thermal expansion coefficient is very similar to that of YAG while that of cubic zirconia is higher. As result, Al_2O_3–YAG binary eutectics are practically free of thermal residual stresses[21] while Al_2O_3 is in compression and YSZ in tension in Al_2O_3–YSZ binary eutectics.[22–24] The R1 and R2 emission bands, corresponding, respectively to the $E(^2E) \rightarrow {}^4A_2$ and $^2A(^2E) \rightarrow {}^4A_2$ transitions of the Cr^{3+} in Al_2O_3 are plotted in Fig. 4 for ternary eutectics grown at 50 mm/h, together with those of an unstressed ruby single crystal. The hydrostatic stress component in the Al_2O_3 domains in the eutectic, σ_h, is obtained from the shift in the R2

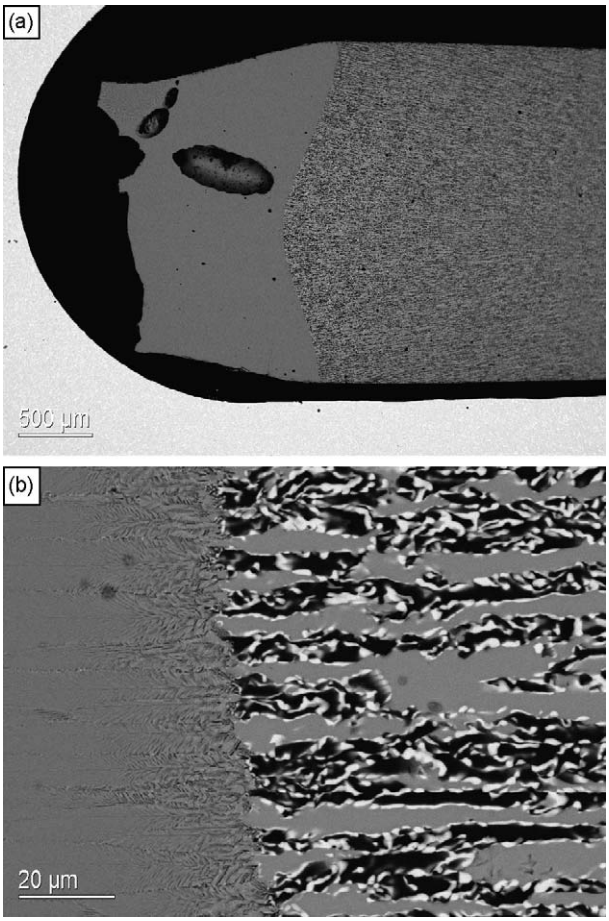

Fig. 3. (a) Back-scattered scanning electro micrograph of the solidification front in a rod grown at 10 mm/h. (b) Detail of the solidification interface in (a). The region at the left side of the solidification front is the air-quenched melt zone. The black phase is alumina, the grey one YAG and the white one YSZ.

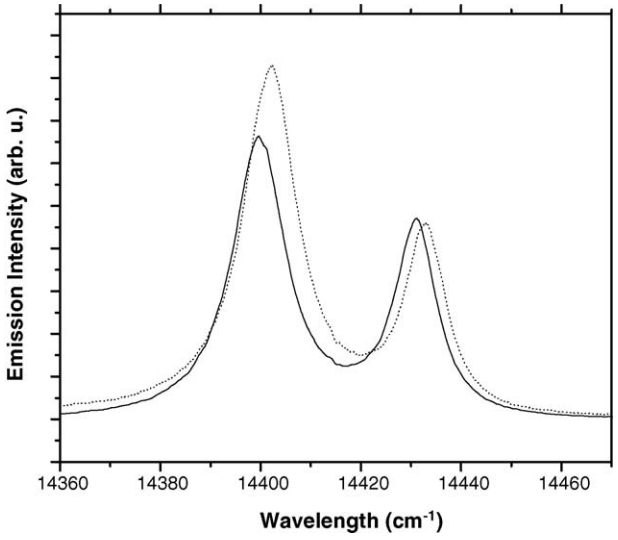

Fig. 4. Cr^{3+} emission spectra of an eutectic rod grown at 50 mm/h (solid line) and unstressed single crystal ruby (broken line). Shifts of the peaks to lower wavelengths correspond to compressive stresses in alumina.

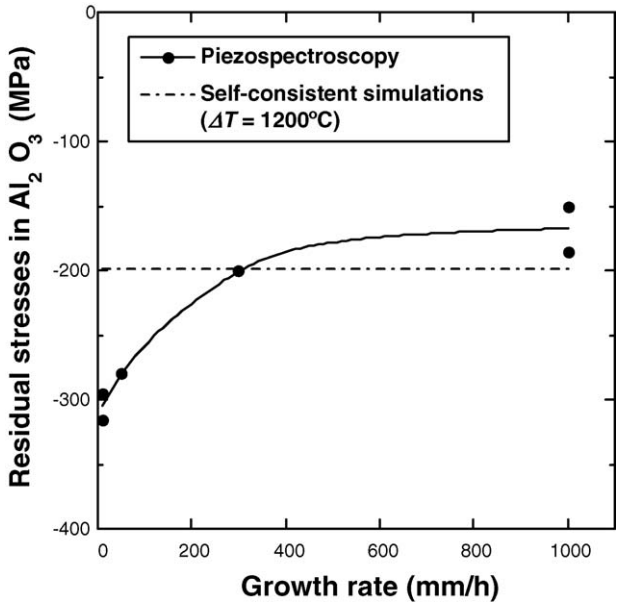

Fig. 5. Thermo-elastic residual stresses at ambient temperature in the Al_2O_3 phase as a function of the growth rate. Experimental results provided by piezospectroscopy and predictions by the self-consistent model.

band peak position $\Delta\nu$ by the scalar relationship.[17]

$$\sigma_h = \frac{\Delta\nu}{7.61} \quad (1)$$

where the stress is expressed in GPa and the shift in cm^{-1}. Alumina was subjected to compressive residual stresses after cooling at room temperature and the average residual stresses in the eutectic rods are plotted as a function of the growth rate in Fig. 5. They were lower than those found in Al_2O_3–YSZ binary eutectics, where alumina was subjected to compressive stresses of ≈400 MPa.[23]

The generation of thermal residual stresses upon cooling from the processing temperature was studied through the self-consistent model. This mean-field approximation, developed to compute the effective elastic properties of polycrystalline solids, is particularly appropriate when the distribution of the various phases leads to an interpenetrating network. All the phases (Al_2O_3, YAG and YSZ) in the eutectic composite were assumed to be perfectly bonded and embedded in an effective medium, whose properties are precisely those of the composite, which are sought. The thermal residual stress tensor in phase i, σ_i, as a result of a homogeneous temperature change ΔT from the stress-free temperature is given by

$$\sigma_i = b_i \Delta T \quad (2)$$

where b_i is the thermal stress concentration tensor of phase i, which is computed as[24]

$$b_i = (I - B_i)[(C^{-1} - C_i^{-1})^{-1}(\sigma_i - \sigma)] \quad (3)$$

where I is the unit tensor of fourth order, and α_i and C_i stand for the thermal expansion coefficient tensor and the elastic stiffness tensor of phase i. Assuming that all the phases behaved as isotropic thermo-elastic solids, these tensors are respectively

Table 1
Elastic modulus, E, Poisson's coefficient, ν, and linear thermal expansion coefficient α

Phase	E (GPa)	ν	α ($K^{-1} \times 10^{-6}$)
Al_2O_3	390	0.27	8.4
YSZ	220	0.29	12.65
YAG	288	0.25	8.0

Data from.[17,22,29–30]

functions of the longitudinal thermal expansion coefficient and of two independent elastic constants, which are given in Table 1. The remaining tensors in Eq. (3) are the mechanical stress concentration tensor of phase i, B_i, and the thermal expansion tensor and the elastic stiffness tensor of the eutectic composite, α and C, which are given by the self-consistent model as[24]

$$B_i = (C_i[I + (S_i C^{-1})(C_i - C)]^{-1})C^{-1}$$
$$C = \sum f_i C[I + (S_i C^{-1})(C_i - C)]^{-1}$$
$$\alpha = \sum f_i B_i \alpha_i \quad (4)$$

where f_i is the volume fraction of phase i and $\boldsymbol{S}_i$ stands for Eshelby's tensor, which depends on the phase shape. To simplify the analyses the simulations assumed that all phases were spherical and the stress free temperature was taken as 1493 K (ΔT = 1200 K) as in previous investigations in Al_2O_3–YSZ binary eutectics.[17,23] The hydrostatic component of the residual stresses in each phase is given in Table 2. The compressive residual stresses in Al_2O_3 are in good agreement with the piezo-spectroscopic results, particularly of the rods grown at higher rates, and they support the thermo-elastic origin of the residual stresses (Fig. 5). Moreover, the self-consistent simulations revealed that the tensile stresses in the YSZ domains were extremely high. The absence of interface cracks in the directionally-solidified eutectics pointed to the excellent interfacial bonding between phases. The piezo-spectroscopic results showed a significant increase in residual stresses in the composite grown at lower rates (≤50 mm/h). There is no clear explanation for this result although it might be related to the differences in the morphology of the microstructure between the rods grown at low and high rates.

3.3. Hardness and fracture toughness

The Vickers hardness measured on the longitudinal sections is plotted in Fig. 6 as a function of the growth rate. The dependence of the hardness on growth rate in our eutectic was slightly lower than that reported on ternary eutectic fibers by Lee et al.[12]

Table 2
Hydrostatic component of the thermal residual stresses in the eutectic phases computed by the self-consistent model

Phase	Residual stress (MPa)
Al_2O_3	−199
YSZ	1130
YAG	−295

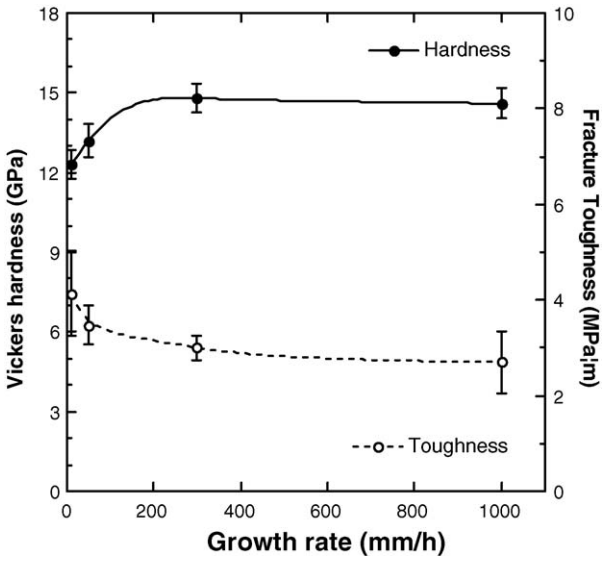

Fig. 6. Vickers hardness and fracture toughness of the ternary eutectic as a function of the growth rate.

These authors reported an increment from 12.4 to 17.5 GPa as the growth rate varied from 60 to 900 mm/h. The fracture toughness was calculated from the Vickers hardness, the eutectic elastic modulus (310 GPa according to the self-consistent model), the crack length l and the indentation diagonal $2a$ using the expression proposed by Niihara for Palmqvist cracks[26] if $l/a \leq 2.5$ or by Anstis[25] for median cracks if $l/a > 2.5$. The results are also plotted in Fig. 6 as a function of the growth rate and showed a slight but noticeable reduction in toughness as the characteristic microstructural size decreased.

It is relevant at this point to compare the results in Fig. 6 with those reported in Al_2O_3/YAG binary eutectic rods processed by the LFZ method at growth rates between 25 and 750 mm/h.[27] The eutectic microstructure was made up of an interpenetrating network of both phases in the proportion 55/45. Higher growth rates also led to a marked reduction in the average thickness of the Al_2O_3 and YAG domains from ≈4 to 0.7 μm but the hardness (≈15–16 GPa) and the fracture toughness (≈2 MPa $m^{1/2}$) were practically independent of the domain size (or growth rate). This was supported by the observation of the fracture micro-mechanisms which showed that the cracks propagated in a straight line from the indentation corners and did not deflect at the interface between the Al_2O_3 and YAG domains. This weak interaction of the crack path with the microstructure was induced by the absence of residual stresses and the excellent bonding between the eutectic phases. On the contrary, crack arrest—followed by the development of another parallel crack a few micrometers above or below the first crack tip—had been observed throughout the crack path in Al_2O_3–YSZ binary eutectics, which presented large thermal residual stresses and higher fracture toughness (≈4–5 MPa $m^{1/2}$).[2,28] The toughness of the ternary eutectics was in between those of Al_2O_3–YAG and Al_2O_3–YSZ, and reduction in the fracture toughness of the ternary eutectics with growth rate could be attributed to a similar mechanism. This was explored by studying the interaction of the crack path with the microstructure in the rods grown at different

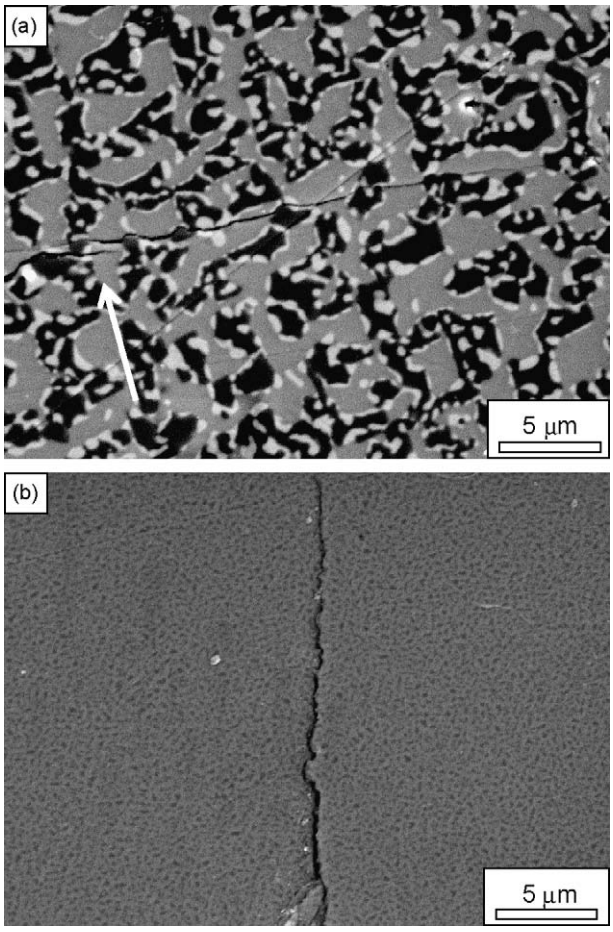

Fig. 7. Back-scattered electron micrographs showing the propagation of a crack through the microstructure in the rods grown at different rates: (a) 50 mm/h and (b) 1000 mm/h. The arrow in (a) points to the arrest of a crack at the YAG/Al_2O_3 interface. The black phase is alumina, the grey one YAG and the white one YSZ.

rates. Representative micrographs of the interaction are shown in Fig. 7a and b of rods grown at 50 and 1000 mm/h. The crack tended to propagate through the YAG phase, which was subjected to tensile residual stresses, and sometimes it was stopped at the YAG/Al_2O_3 interface and a new crack was initiated nearby (Fig. 7a). The interactions of the crack path with the microstructure were more difficult to detect in the rods grown at higher rates because of the submicron domain size, but the meandering crack profile shown in Fig. 7b is indicative that the direction of crack propagation at the microscopic level was influenced by the microstructure. Of course, crack deflection and crack arrest were more pronounced in the eutectics with larger domain size, and led to the reduction in toughness with growth rate observed in Fig. 6.

3.4. Flexure strength

Recent experimental data on the Al_2O_3/YAG binary system have demonstrated that the flexure strength of eutectics with an interpenetrating microstructure increased as the domain size decreases.[26] Hence, the best mechanical properties were expected in the rods grown at higher rates, which also presented more porosity. The best compromise between porosity and domain size was reached in the ternary eutectic rods grown at 300 mm/h, whose flexure strength is plotted as a function of the test temperature in Fig. 8. The ambient temperature results showed a lot of scatter due to the presence of voids and pores in the rods which acted as stress concentrators, but the average value was impressive, showing the outstanding strength of this ternary eutectic, which is higher than the maximum values reported for Al_2O_3/YAG (1.9 GPa in[26]) and Al_2O_3/YSZ (1.6 GPA in[3]) processed and tested under the same conditions. The flexure strength of Al_2O_3/YAG binary eutectics grown at 350 mm/h is also plotted in Fig. 8, as it demonstrates the advantages and limitations of the ternary eutectic system as compared with the binary one. The presence of the small YSZ domains in the ternary eutectic led to a significant reduction in the average domain size (from 1 μm in Al_2O_3/YAG to 0.35 μm Al_2O_3/YAG/YSZ). The eutectic strength is controlled by the average defect size which, in turn, is related to the domain size if the microstructure is homogeneous. As a result, the ambient temperature strength of ternary eutectic was twice higher than that of the binary system grown at the same rate.

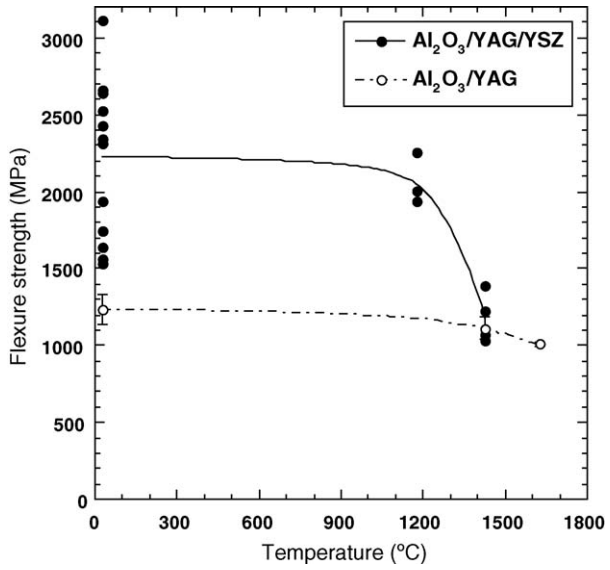

Fig. 8. Influence of temperature on the flexure strength of Al_2O_3/YAG/YSZ ternary eutectic rods grown at 300 mm/h. The behavior of an Al_2O_3/YAG binary eutectic grown at 350 mm/h is also plotted for comparison.[26]

The susceptibility of the ternary eutectic to pores and other imperfections was reduced at high temperature, as plastic deformation around the pores smoothed out the stress concentration. However, the flexure strength of the ternary system dropped rapidly above 1473 K, being reduced to one half of the ambient temperature value at 1700 K. This contrasts with the behaviour of the Al_2O_3/YAG binary eutectic, which retained the ambient temperature strength up to 1873 K. The excellent strength retention of the binary Al_2O_3/YAG eutectics was attributed to the combination of the creep resistance of YAG with the microstructure stability of the system, which presented very little coarsening after short-term exposure at 1900 K. Al_2O_3/YAG/YSZ exhibits two mechanisms, which may explain, at least partially, the strength

degradation at high temperature and which are not present in the Al_2O_3/YAG eutectic system. The first is the relief of the thermal residual stresses at high temperature, which leads to better crack growth resistance at ambient temperature as they promote crack arrest and deflection.[28,31] The second is the plastic deformation of YSZ above 1473 K, which is well documented in the literature and can also lead to a reduction in the eutectic strength above this temperature. Finally, the extremely fine domain size in the ternary eutectics (0.35 μm) will enhance the activation of diffusion-assisted deformation mechanisms which are not critical in binary eutectics with larger domain size, where plastic deformation at high temperature is controlled by dislocation movement.[13] It should be noted, however, that even if the strength retention of the Al_2O_3/YAG/YSZ is poor in comparison with that of binary systems, the ternary eutectic presents an extraordinary ambient temperature strength, which is still equal to or even higher than that of the binary eutectics at 1673 K.

4. Summary

Directionally-solidified rods of Al_2O_3/YAG/ZrO_2 ternary eutectic were manufactured by the LFZ under different growth conditions. The rods presented a Chinese script microstructure formed by an interpenetrating network of Al_2O_3 (40%) and YAG (42%) domains of similar size with smaller YSZ (18%) domains at the Al_2O_3/YAG interfaces. The domain size decreased and the solidification front became flatter with the growth rate, leading to more homogeneous microstructures. Precursor rotation did not modify, however, the domain size nor improve the homogeneity. Elongated pores were always found within the rods at solidification rates above 300 mm/h. Thermo-elastic residual stresses developed upon cooling due to thermal expansion mismatch of the phases; they were compressive in Al_2O_3 (as shown by piezo-spectroscopic measurements) and tensile in YAG and YSZ (as indicated by the self-consistent simulations). The hardness increased and the fracture toughness decreased with the growth rate, and maximum values of 14.8 GPa and 4.3 MPa $m^{1/2}$, respectively, were measured. The ternary Al_2O_3/YAG/YSZ eutectic presented a much finer microstructure size than did binary Al_2O_3/YAG eutectics grown at the same rate, and as a result, the flexure strength of the rods grown at 300 mm/h was higher and reached an average value of 2.2 GPa. The ternary eutectic showed good strength retention up to 1473 K but the flexure was reduced to one half at 1700 K, which is still comparable to the best binary eutectics of the Al_2O_3–YAG system. The relationship between the microstructure and the mechanical properties and the possible causes of the strength degradation above 1473 K were discussed.

Acknowledgements

The authors gratefully acknowledge the financial support from the Spanish Ministry of Science and Education (SMST) under project MAT2003-06085-C03-01 and from the Autonomous Government of Madrid though grant GR/MAT/357/2004.

References

1. Orera, V. M. and Llorca, J., *Directionally Solidified Eutectic Oxide Ceramics in the Encyclopedia of Materials: Science and Technology*. Elsevier, 2005.
2. Llorca, J., Pastor, J. Y., Poza, P., Peña, J. I., de Francisco, I., Larrea, A. *et al.*, Influence of the Y_2O_3 content and temperature on the mechanical properties of melt-grown Al_2O_3–ZrO_2 eutectics. *J. Am. Ceram. Soc.*, 2004, **87**, 633–639.
3. Pastor, J. Y., Llorca, J., Poza, P., de Francisco, I., Merino, R. I. and Peña, J. I., Mechanical properties of melt grown Al_2O_3–$ZrO_2(Y_2O_3)$ eutectics with different microstructure. *J. Eur. Ceram. Soc.*, 2005, **25**, 1215.
4. Sayir, A. and Farmer, S. C., The effect of the microstructure on mechanical properties of directionally solidified $Al_2O_3/ZrO_2(Y_2O_3)$ eutectic. *Acta Mater.*, 2000, **48**, 4691–4697.
5. Ochiai, S., Ueda, T., Sato, K., Hojo, M., Waku, Y., Nakagawa, N. *et al.*, Deformation and fracture behavior of an Al_2O_3/YAG composite from room temperature to 2023K. *Compos. Sci. Technol.*, 2001, **61**, 2117–2128.
6. Waku, Y. and Sakuma, T., Dislocation mechanism of deformation and strength of Al_2O_3–YAG single crystal composites at high temperatures above 1500 °C. *J. Eur. Ceram. Soc.*, 2000, **20**, 1453–1458.
7. Larrea, A., de la Fuente, G. F., Merino, R. I. and Orera, V. M., ZrO_2–Al_2O_3 eutectic plates produced by laser zone melting. *J. Eur. Ceram. Soc.*, 2002, **22**, 191–198.
8. Peña, J. I., Merino, R. I., Harlan, N. R., Larrea, A., de la Fuente, G. F. and Orera, V. M., Microstructure of Y_2O_3 doped Al_2O_3–ZrO_2 eutectics grown by the laser floating-zone melted. *J. Eur. Ceram. Soc.*, 2002, **22**, 2595–2602.
9. Starostin, M. Y., Gnesin, B. A. and Yalovets, T. N., Microstructure and crystallographic phase textures of the alumina–zirconia eutectics. *J. Cryst. Growth*, 1997, **171**, 119–124.
10. Yasuda, H., Ohnaka, I., Mizutani, Y., Sugiyama, A., Morikawa, T., Takeshima, S. *et al.*, Solidification and shape casting of Al_2O_3–YAG eutectic ceramics from the undercooled melt produced by melting Al_2O_3–YAP eutectics. *Sci. Technol. Adv. Mater.*, 2004, **5**, 207–217.
11. Calderon-Moreno, J. M. and Yoshimura, M., Effect of melt quenching on the subsolidus equilibria in the ternary system Al_2O_3–$Y_3Al_5O_{12}$–ZrO_2. *Solid State Ionics*, 2001, **142**, 343–349.
12. Lee, J. H., Yoshikawa, A., Fukuda, T. and Waku, Y., Growth and characterization of $Al_2O_3/Y_3Al_5O_{12}/ZrO_2$ ternary eutectic fibers. *J. Cryst. Growth*, 2001, **231**, 115–120.
13. Waku, Y., Sakata, S., Mitani, A., Shimizu, K. and Hasebe, M., Temperature dependence of flexural strength and microstructure of Al_2O_3–$Y_3Al_5O_{12}$–ZrO_2 ternary melt growth composites. *J. Mater. Sci.*, 2002, **37**, 2975–2982.
14. Lakiza, S. M. and Lopato, L. M., Stable and metastable phase relations in the system alumina–zirconia–yttria. *J. Am. Ceram. Soc.*, 1997, **80**, 893–902.
15. Peña, J. I., Merino, R. I., de la Fuente, G. F. and Orera, V. M., Aligned ZrO_2(c)–$CaZrO_3$ eutectics grown by the laser floating-zone method: electrical and optical properties. *Adv. Mater.*, 1996, **8**, 909–912.
16. Riedel, R., *Handbook of Ceramic Hard Materials*, *1*. Wiley–VCH Verlag GmbH, Weinheim, 2000.
17. Pardo, J. A., Merino, R. I., Orera, V. M., Peña, J. I., González, C., Pastor, J. Y. *et al.*, Piezo-spectroscopic study of residual stresses in Al_2O_3–$ZrO_2(Y_2O_3)$ directionally solidified eutectics. *J. Am. Ceram. Soc.*, 2000, **83**, 2745–2752.
18. Fratello, V. J. and Brandle, C. D., Physical properties of a YAG melt. *J. Cryst. Growth*, 1993, **128**, 1006–1010.
19. Young, G. W. and Chait, A., Steady-state thermal-solutal diffusion in a float zone. *J. Cryst. Growth*, 1989, **96**, 65–95.
20. de Francisco, I., Orera, V.M., Merino, R.I., Larrea, A. and Peña, J.I., Growth of Al2O3–ZrO2(Y2O3) eutectic rods by the laser floating-zone technique: effect of the rotation. *J. Eur. Ceram. Soc.*, in press.
21. Dickey, E. C., Frazer, C. S., Watkins, T. R. and Hubbard, C. R., Residual stresses in high-temperature ceramic eutectics. *J. Eur. Ceram. Soc.*, 1999, **19**, 2503–2509.

22. Orera, V. M., Cemborain, R., Merino, R. I., Peña, J. I. and Larrea, A., Piezo-spectroscopy at low temperatures: residual stresses in Al_2O_3–$ZrO_2(Y_2O_3)$ eutectics measured from 77 to 350 K. *Acta Mater*, 2002, **50**, 4677–4686.
23. Harlan, N. R., Merino, R. I., Peña, J. I., Larrea, A., Orera, V. M., Gonzalez, C. *et al.*, Phase distribution and residual stresses in melt-grown Al_2O_3–$ZrO_2(Y_2O_3)$ eutectics. *J. Am. Ceram. Soc.*, 2002, **85**, 2025–2032.
24. Benveniste, Y., Dvorak, G. J. and Chen, T., On diagonal and elastic symmetry of the approximate effective stiffness tensor of heterogeneous media. *J. Mech. Phys. Solids*, 1991, **39**, 927–946.
25. Niihara, K., A fracture-mechanics analysis of indentation-induced Palmqvist crack in ceramics. *J. Mater Sci.*, 1983, **2**, 221–223.
26. Anstis, G. R., Chantikul, P., Lawn, B. R. and Marshall, D. B., A critical evaluation of indentation techniques for measuring fracture toughness: I, direct crack measurements. *J. Am. Ceram. Soc.*, 1981, **64**, 533–538.
27. Pastor, J. Y., Llorca, J., Salazar, A., Oliete, P. B., de Francisco, I. and Peña, J. I., Mechanical properties of melt-grown alumina–YAG eutectics up to 1900 K. *J. Am. Ceram. Soc.*, 2005, **88**, 1488.
28. Pastor, J. Y., Poza, P., Llorca, J., Peña, J. I., Merino, R. I. and Orera, V. M., Mechanical properties of directionally solidified Al_2O_3–$ZrO_2(Y_2O_3)$ eutectics. *Mater. Sci. Eng. A*, 2001, **308**, 241–249.
29. Alton, W. J. and Barlow, A. J., Temperature dependence of the elastic constants of yttrium aluminum garnet. *J. Appl. Phys.*, 1967, **38**(7), 3023–3024.
30. Handbook, of Laser Science and Technology, p. 329.
31. Orera, V. M., Merino, R. I., Pardo, J. A., Larrea, A., Peña, J. I., González, C. *et al.*, Microstructure and physical properties of some eutectic composites processed by directional solidification. *Acta Materialia*, 2000, **48**, 4683–4689.